Diagonal and Skewed Parton Distributions

A.D. Martin

University of Durham, Durham, DH1 3LE, UK

Abstract. We briefly review the global analyses that are used to determine parton distributions from data, and discuss recent topical issues that have arisen. We outline the properties of skewed parton distributions, and show that in the small x domain they are completely determined by the conventional distributions. The relevance to the description of vector meson production at HERA is emphasized.

1 Introduction

The cross section of hard scattering processes involving incoming protons (such as deep inelastic electron-proton scattering or the hadroproduction of jets of large transverse momentum) can be written as the sum of parton distributions multiplied by the cross sections of hard subprocesses calculated at the parton level using perturbative QCD. That is we can factor off the long distance (non-perturbative) effects into universal, process independent, parton distributions, $f_i(x,\mu^2)$ with $i = q, \bar{q}, g$, which represent the probability of finding parton i in the proton carrying a longitudinal fraction x of the proton's momentum. The parameter μ is a scale typical of the hard partonic subprocesses. Perturbative QCD determines the evolution of the parton distributions as a function of μ, provided they are known as some starting scale μ_0. Calculating the parton distributions from first principles at some low scale μ_0 is one of the most challenging problems of non-perturbative QCD. The most promising approach is lattice QCD, but much remains to be done. On the other hand, from a practical point of view, the parton distributions of the proton are determined with good precision from global analyses of deep inelastic and related hard scattering data. We will describe these analyses in Section 2 and focus on some of the recent issues that result.

Formally parton distributions can be expressed as matrix elements $\langle p|\hat{O}|p\rangle$ where $\hat{O}$ is a twist-2 quark or gluon operator, and p is the four momentum of the proton. Recently there has been much renewed interest in off-diagonal or skewed parton distributions which are given by matrix elements $\langle p'|\hat{O}|p\rangle$ in which the momentum p' of the outgoing proton is not the same as that of the incoming proton. For example, the *amplitudes* for processes such as deeply virtual Compton scattering ($\gamma^* p \to \gamma p$) or vector particle electro- or photo-production ($\gamma^* p \to Zp$ or $J/\psi p$) depend on off-diagonal distributions. Since $p \neq p'$ the parton returning to the proton has a different momentum to the one which is outgoing, and so we need two momentum variables to specify the skewed

distributions. In Section 3 we will discuss the phenomenological developments involving skewed distributions (concentrating entirely on the small x domain) and emphasize their potential role in the global parton analyses.

2 Global parton analyses

As mentioned above, the parton densities $f_i(x,Q^2)$ are determined from a global analysis of a wide range of data for deep inelastic and related 'hard' scattering processes, which are listed in the first column of Table 1. The procedure is to parametrize the x dependence of the 'starting' distributions in physically motivated forms, such as

$$xf_i(x,Q_0^2) \;=\; A_i x^{-\alpha_i}(1-x)^{\beta_i}(1+\gamma_i x^{\frac{1}{2}}+\delta_i x) \tag{1}$$

at a low scale Q_0^2, but which is nevertheless sufficiently high to be in the perturbative region. Next-to-leading order DGLAP equations are then used to evolve up in Q^2 to determine $f_i(x,Q^2)$ at all the x,Q^2 at which data are to be fitted, and the parameters $A_i,\alpha_i,\ldots\delta_i$ varied until an optimum description of the data is achieved, subject to satisfying the momentum and flavour sum rules. The last column of Table 1 gives an indication of the parton properties that are constrained by particular data sets. Two independent groups have carried out global analyses: MRST and CTEQ. Their latest sets of partons are known as MRST [1], MRST99 [2] and CTEQ5 [3]. Semi-global analyses are also being undertaken by the experimental collaborations (see, for example, [4]). In this section we review topical issues concerning these global parton analyses. We adopt the conventional notation $u\equiv f_u, d\equiv f_d$ etc.

2.1 Light quark distributions: u, d, s

The u and d distributions are pinned down by the DIS data, with the slope of d/u being constrained for $x\lesssim 0.3$ by the CDF $W^\pm$ rapidity asymmetry data. In fact d/u is determined up to $x\sim 0.7$ by the NMC F_2^n/F_2^p data, *provided* that we assume that there are no deuterium binding corrections for $x>0.3$. However, Yang and Bodek [5] have recently stressed a point made by Melnitchouk and Thomas [6] that the F_2^n data may have a nuclear binding correction which would lead to a larger d/u ratio at large x. This leads to considerable uncertainty in the d distribution at large x. Descriptions with $d/u\to 0$ or 0.2 as $x\to 1$ are equally possible. In principle measurements of charged current DIS $e^+p\to\bar\nu X$ (and $e^-p\to\nu X$) at HERA, or $W^\pm$ asymmetry at large rapidity at the LHC, can resolve the issue [2].

The ratio $\bar d/\bar u$ of sea quark distributions is determined for $0.05\lesssim x\lesssim 0.3$ by the E866 data for $pp,pn\to\mu^+\mu^-X$ [10]. Information is also coming from the HERMES data for $ep,en\to e\pi^\pm X$. It is found that $\bar d/\bar u$ rises from unity at $x=0$ to about 1.5 at $x=0.15$ and then falls sharply back through unity around $x\sim 0.3$.

Table 1. Processes studied in global analyses. The essential features of the partons that are probed by the particular data sets are indicated in the last column.

Process/ Experiment	**Leading order subprocess**	**Parton behaviour probed**
DIS ($\mu N \to \mu X$) $F_2^{\mu p}, F_2^{\mu d}, F_2^{\mu n}/F_2^{\mu p}$ (SLAC, BCDMS, NMC, E665)	$\gamma^* q \to q$	Four structure functions $\to$ $u+\bar{u}$, $d+\bar{d}$, $\bar{u}+\bar{d}$, s (assumed $=\bar{s}$), but only $\int xg(x,Q_0^2)dx \simeq 0.35$ and $\int(\bar{d}-\bar{u})dx \simeq 0.1$
DIS ($\nu N \to \mu X$) $F_2^{\nu N}, xF_3^{\nu N}$ (CCFR)	$W^* q \to q'$	
DIS (small x) F_2^{ep} (H1, ZEUS)	$\gamma^*(Z^*)q \to q$	λ $(x\bar{q} \sim x^{-\lambda_S},\ xg \sim x^{-\lambda_g})$
DIS (F_L) NMC, HERA	$\gamma^* g \to q\bar{q}$	g
$\ell N \to c\bar{c}X$ F_2^c (EMC; H1, ZEUS)	$\gamma^* c \to c$	c $(x \gtrsim 0.01;\ x \lesssim 0.01)$
$\nu N \to \mu^+\mu^- X$ (CCFR)	$W^* s \to c$ $\hookrightarrow \mu^+$	$s \approx \frac{1}{4}(\bar{u}+\bar{d})$
$pN \to \gamma X$ (WA70, UA6, E706, ...)	$qg \to \gamma q$	g at $x \simeq 2p_T^\gamma/\sqrt{s} \to$ $x \approx 0.2-0.6$
$pN \to \mu^+\mu^- X$ (E605, E772)	$q\bar{q} \to \gamma^*$	$\bar{q} = ...(1-x)^{\eta_S}$
$pp, pn \to \mu^+\mu^- X$ (E866, NA51)	$u\bar{u}, d\bar{d} \to \gamma^*$ $u\bar{d}, d\bar{u} \to \gamma^*$	$\bar{u}-\bar{d}$ $(0.04 \lesssim x \lesssim 0.3)$
$ep, en \to e\pi X$ (HERMES)	$\gamma^* q \to q$ with $q = u, d, \bar{u}, \bar{d}$	$\bar{u}-\bar{d}$ $(0.04 \lesssim x \lesssim 0.2)$
$p\bar{p} \to WX(ZX)$ (UA1, UA2; CDF, D0)	$ud \to W$	u, d at $x \simeq M_W/\sqrt{s} \to$ $x \approx 0.13;\ 0.05$
$\to \ell^\pm$ asym (CDF)		slope of u/d at $x \approx 0.05-0.1$
$p\bar{p} \to t\bar{t}X$ (CDF, D0)	$q\bar{q}, gg \to t\bar{t}$	q, g at $x \gtrsim 2m_t/\sqrt{s} \simeq 0.2$
$p\bar{p} \to$ jet $+ X$ (CDF, D0)	$gg, qg, qq \to 2j$	q, g at $x \simeq 2E_T/\sqrt{s} \to$ $x \approx 0.05-0.5$

In principle $\nu N \to \mu^- X$ and $\bar{\nu} N \to \mu^+ X$ DIS data can determine s and $\bar{s}$ distributions separately. However so far the global analyses have used the studies of the CCFR dimuon production data, which yields

$$s + \bar{s} \simeq (\bar{u} + \bar{d})/2 \tag{2}$$

independent of x at $Q^2 = 1$ GeV^2, with typically a $\pm 10\%$ error [2].

2.2 Heavy quark distributions: *c* and *b*

The improved theoretical treatments have recently enabled these distributions to be put on a sound basis in the global analyses (see, for example, [7]). For a heavy quark distribution (say c) we should match, at $Q^2 = m_c^2$, the fixed flavour number scheme, describing $\gamma g \to c\bar{c}$ with $n_f = 3$ to the variable flavour number scheme with $n_f = 4$ flavours for $Q^2 > m_c^2$. MRST [1] use the Thorne-Roberts prescription [8] in which F_2^c and $\partial F_2^c / \partial \ln Q^2$ are required to be continuous at $Q^2 = m_c^2$, whereas CTEQ [3] use an alternative 'ACOT' prescription [9]. In this way the charm distribution is generated perturbatively with the mass of the charm quark m_c as the only free parameter. Not surprisingly, due to the $g \to c\bar{c}$ transition, the charm distribution mirrors the form of the gluon distribution. At some level we may expect an 'intrinsic' component of the charm distribution.

2.3 The gluon distribution *g*

In principle many processes are sensitive to the gluon distribution, but it is still difficult to determine for $x \gtrsim 0.2$ where it becomes increasingly small. In this region MRST [1] used the WA70 prompt photon data to determine the gluon. However this process suffers from scale dependence (reflecting the higher order corrections), effects of intrinsic k_T (needed to describe the E706 prompt photon data) and uncertainties due to fragmentation effects and isolation criteria. In an attempt to provide an acceptable spread of gluon distributions at large x, MRST presented three sets of partons ($g \uparrow$, the default MRST set, $g \downarrow$) corresponding, respectively, to an average intrinsic $k_T = 0, 0.4$ and 0.64 GeV for the WA70 data. The arrows indicate the relative sizes of the gluons in the large x region. The corresponding $\langle k_T \rangle$ needed to obtain a good description of the E706 prompt photon data is worryingly large at about 1 GeV.

Due to the uncertainties associated with prompt photon production, the recent CTEQ analysis [3] omits these data and instead determines the large x behaviour of the gluon using the single jet inclusive E_T distributions measured at the Tevatron. The above three MRST sets of partons 'predict' the shape of the jet E_T distributions remarkably well, but the predicted normalization is 7%, 13%, 17% below the data respectively with $g \uparrow$ being closest to CTEQ5.

Turning now to the small x domain, the gluon is well constrained by the observed behaviour of $\partial F_2 / \partial \log Q^2$. To be precise the H1 and ZEUS data determine the gluon for $x \lesssim 0.01$, and the NMC data for $x \lesssim 0.1$. Inspection of F_2

as a function of $\ln Q^2$ at low fixed x [11,4] shows that the data flatten out at low Q^2, indicating a smaller value of

$$\partial F_2/\partial \ln Q^2 \simeq \alpha_S(Q^2) P_{gg} \otimes g. \tag{3}$$

Also α_S increases with decreasing Q^2, and as a consequence $g(x)$ becomes valence-like for $Q^2 \simeq 1$ GeV^2, which is about the lowest value of Q^2 for a DGLAP description. In fact $Q^2 \simeq 2$ GeV^2, where the gluon becomes flat (that is $g(x) \to$ constant as $x \to 0$), is a more reasonable lower limit for DGLAP evolution.

2.4 *W* production at the Tevatron and the LHC

The total cross sections for W and Z hadroproduction are known to NNLO [12] and the input electroweak parameters are known to high accuracy. The main uncertainty in predicting the size of the cross sections comes from the parton distributions and, to a lesser extent, from the value of α_S. The MRST predictions are [2]

$$B(W \to \ell\nu)\sigma_W \;=\; \begin{cases} 2.45 \text{ nb } (\pm 3\%) \text{ at the Tevatron} \\ 20.3 \text{ nb } (\pm 5\%) \text{ at the LHC.} \end{cases} \tag{4}$$

The errors arise from considering the spread of predictions arising from taking the full range of parton sets, including a ± 0.005 uncertainty in $\alpha_S(M_Z^2)$. In principle the predictions allow a check on the luminosity of the collider. Of course, there are uncertainties in the parton distributions due to the normalization errors on present data. To make an attempt to allow for this, the range of parton sets used to specify the errors in (4) includes sets obtained from global fits with the HERA deep inelastic data renormalized up by 2.5%, and then down by 2.5%.

2.5 Comparison of MRST and CTEQ partons

The predictions for σ_W serve another purpose. The long evolution length to $Q^2 = M_W^2$, together with the expected precision of the predictions, can expose small defects in the evolution codes used the global analyses. An unexpectedly large difference was found between the cross sections predicted using MRST98 [1] and CTEQ5 [3] partons. The value for σ_W obtained from CTEQ5 was 10% greater than from MRST98 partons at the LHC energy. It means that the evolution codes should be carefully checked. Recall that neither CTEQ, nor MRS, agreed completely with the "standard HERA workshop code [13]" for a test evolution from $Q^2 = 4$ to 100 GeV^2. In the interval $10^{-4} \lesssim x \lesssim 10^{-1}$, the CTEQ sea was some 4% high, and the MRS sea was 1% low and the gluon about 1.5% low. MRST checked their code and found that it had to be corrected by a factor $C_F \to C_A$ in one of the terms appearing in the NLO P_{gg} splitting function. The effect is to make the gluon, and hence the sea, evolve a little more rapidly at small x. With the correction the MRST99 code [2] is found to agree precisely with the "standard" evolution code and, moreover, is consistent with exact momentum conservation as a function of Q^2, as it should be. However the discrepancy for

σ_W remains: the CTEQ5 HQ prediction is about 6% (10%) higher at Tevatron (LHC) energies [2]. Differences between MRST and CTEQ partons can arise from the choice of the data sets to be included in the global fit, the Q^2, W^2 cuts used, the different renormalization of some data sets, the different treatment of heavy flavours, etc. However none of these differences appears sufficient to explain the discrepancy in the predictions for σ_W, which sample partons at $Q^2 = M_W^2$ with $x \simeq M_W/\sqrt{s}$.

2.6 Outstanding problems of global analyses

There is a need to determine realistic errors on the parton distributions extracted in a global analysis. This is far from easy. In particular, among other things, we need to quantify the uncertainties due to (i) heavy target and other nuclear corrections, (ii) the possible effects of higher twist contributions, (iii) the choice of the form of parametrization of the initial distributions, and (iv) the possible effects of k_T smearing on the analysis of exclusive processes.

A second, and related, problem is the need for a next-to-next-leading order (NNLO) analysis. The P_{gg} splitting function is not yet known to this order. Also, as data at smaller and smaller x are included, there is a need to resum $\log(1/x)$ effects, and to allow for parton shadowing corrections.

3 Skewed (or off-diagonal) parton distributions

Data of higher and higher precision are becoming available for processes which are described by off-diagonal (or skewed) parton distributions in the small x domain. A relevant example is diffractive vector meson production at HERA, $\gamma^* p \to Vp$ with $V = \rho, J/\psi$ or Υ (see, for example, [14]). At high $\gamma^* p$ c.m. energy, W, the cross section is dominated by the two-gluon exchange amplitude

$$\left.\frac{d\sigma}{dt}(\gamma^* p \to Vp)\right|_{t=0} = \ldots [x_2 g(x_1, x_2, \mu^2)]^2 \tag{5}$$

where g is the off-diagonal ($x_1 \neq x_2$) gluon distribution with

$$\begin{aligned} x_1 &= (Q^2 + M_{q\bar{q}}^2)/W^2, \\ x_2 &= (M_{q\bar{q}}^2 - M_V^2)/W^2 \ll x_1, \end{aligned} \tag{6}$$

see [15]. The process is shown schematically in Fig. 1. $M_{q\bar{q}}$ is the mass of the $q\bar{q}$ system produced by a photon of virtuality Q^2. The relevant scale is $\mu^2 = z(1-z)Q^2 + k_T^2 + m_q^2$ where $z, 1-z$ and $\pm \boldsymbol{k}_T$ specify the momenta of the q and $\bar{q}$ which form the vector meson of mass M_V. The quadratic dependence of g in (5) shows that these data may offer a sensitive constraint on the gluon. Indeed we will see that the off-diagonal distributions are fixed by the conventional (diagonal) parton distributions of Section 2, so that the data can, in principle, be included in a global parton analysis.

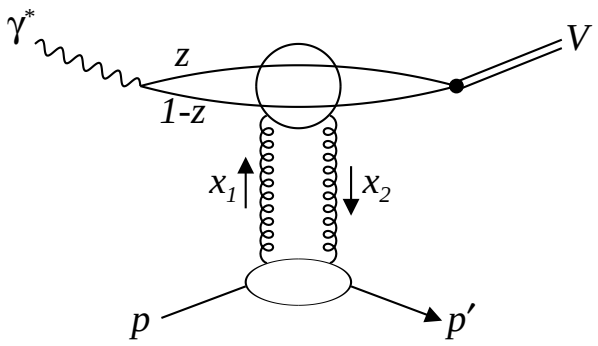

Fig. 1. Schematic diagram for diffractive vector meson production at HERA, $\gamma^* p \to Vp$. The longitudinal fractions x_1 and x_2 of the in going and out going proton momentum are given by (6). z and $1-z$ are the longitudinal fractions of the q and $\bar{q}$ momenta. There are four possible couplings of the two gluons to the q and $\bar{q}$, represented by the upper circle.

3.1 Ji's symmetrized distributions

It is convenient to use the skewed parton distributions $H(x,\xi) \equiv H(x,\xi,t,\mu^2)$, with support $-1 \le x \le 1$, introduced by Ji [16], with the minor difference that the gluon $H_g = xH_g^{\rm Ji}$ [17]. The distributions depend on the momentum fractions

$$x_{1.2} \;=\; x \pm \xi \tag{7}$$

carried by the emitted and absorbed partons at each scale μ^2, and on the momentum transfer variable $t = (p-p')^2$. The variables do not change as we evolve the distributions up in the scale μ^2. In the limit $\xi \to 0$ they reduce to the conventional parton distributions

$$\begin{aligned} H_q(x,0) &= \begin{cases} q(x) & \text{for } x > 0 \\ -\bar{q}(-x) & \text{for } x < 0 \end{cases} \\ H_g(x,0) &= xg(x), \end{aligned} \tag{8}$$

and satisfy DGLAP evolution. In the limit $\xi \to 1$ they obey ERBL evolution [18,19]. If we consider H_q at arbitrary values of ξ, then for $x > \xi$ and $x < -\xi$ we have DGLAP-like evolution for quarks and antiquarks respectively, while for $-\xi < x < \xi$ we have ERBL-like evolution for the emitted $q\bar{q}$ pair.

On account of the $x_1 \leftrightarrow x_2$ symmetry the distributions H_q and H_g are symmetric in ξ

$$H_i(x,\xi) \;=\; H_i(x,-\xi). \tag{9}$$

We also have symmetry relations in terms of the x variable

$$\begin{aligned} H_q^{NS}(x,\xi) &= H_q^{NS}(-x,\xi) \\ H_q^{S}(x,\xi) &= -H_q^{S}(-x,\xi) \\ H_g(x,\xi) &= H_g(-x,\xi) \end{aligned} \tag{10}$$

where the superscripts S and NS denote singlet and non-singlet quarks respectively.

3.2 $H(x,\xi)$ in terms of conformal moments

In order to relate the skewed distributions to the conventional parton densities it is convenient to work in terms of the so-called conformal moments[1] of the skewed distributions

$$\boxed{O_N(\xi,\mu^2) \;=\; \int_{-1}^{1} dx R_N(x_1,x_2) H(x,\xi,\mu^2).} \tag{11}$$

At leading order, these moments are not mixed by evolution. In fact

$$O_N(\xi,\mu^2) \;=\; O_N(\xi,\mu_0^2)\left(\frac{\mu^2}{\mu_0^2}\right)^{\gamma_N}, \tag{12}$$

where γ_N are the same anomalous dimensions as for diagonal partons. The R_N are known polynomials of degree N

$$R_N \;=\; \sum_{k=0}^{N} \binom{N}{k} \binom{N+2p}{k+p} x_1^k x_2^{N-k} \tag{13}$$

with $p = 1, 2$ for quarks and gluons respectively. The O_N reduce to the usual moments in the limit $\xi \to 0$. For example for quarks

$$O_N \to M_N \;=\; \int_0^1 x^N q(x) dx, \tag{14}$$

up to a normalizing factor $R_N(1,1)$.

The crucial step is to find the inverse relation to (11). That is to reconstruct $H(x,\xi)$ from a knowledge of its conformal moments. The result, due to Shuvaev [23], is

$$\boxed{H(x,\xi) \;=\; \int_{-1}^{1} dx' K(x,\xi;x') f(x')} \tag{15}$$

where the kernel K is a known integral [23,24] and f is the Mellin transform

$$f(x') \;=\; \int \frac{dN}{2\pi i} (x')^{-N} O_N(\xi)/R_N(1,1). \tag{16}$$

[1] Conformal moments were introduced in [18,20] for $\xi = 1$, and in [21] for $\xi \neq 1$; see also [22].

The function f reduces to the conventional diagonal parton distribution for $\xi^2 \ll 1$. This follows since [16]

$$O_N(\xi) = \sum_{k=0}^{[(N+1)/2]} O_{Nk}\xi^{2k}$$
$$\simeq O_{N0} \;=\; O_N(0) = M_N R_N(1,1) \tag{17}$$

for small ξ^2. So the skewed distribution H is completely determined in terms of the diagonal distribution f via (15). This identification can be made at any scale, and so there is no need to solve the off-diagonal evolution equations to obtain the μ^2 dependence of $H(x,\xi,\mu^2)$. That is the normal DGLAP evolution of $f(x,\mu^2)$ is sufficient to generate the x,ξ and μ^2 dependence of $H(x,\xi,\mu^2)$ at small x and ξ.

3.3 A good small x,ξ approximation

We can simplify (15) further if we assume that the diagonal partons have the forms

$$xq(x) \;=\; N_q x^{-\lambda_q}, \quad xg(x) \;=\; N_g x^{-\lambda_g}, \tag{18}$$

which should be valid for very small x. Then the x' integration in (15) can be performed analytically, giving

$$H_i(x,\xi) \;=\; \xi^{-\lambda_i - p} F_i\left(\frac{x}{\xi}\right) \tag{19}$$

with $p = 1, 0$ for $i = q, g$ respectively, where the F_i are known in terms of N_i and λ_i. A full set of results can be found in [24] for the off-diagonal/diagonal ratios,

$$R_i(x,\xi) \;=\; H_i(x,\xi)/H_i(x+\xi,0), \tag{20}$$

for which the only free parameter is λ_i. In [24] the ratios $R_q^{NS,S}$ and R_g are plotted as functions of x/ξ for different values of λ_i. The scale dependence of the off-diagonal distributions, $H_i(x,\xi)$ of (19), and hence of the R_i, is hidden in the μ^2 dependence of the λ_i. Both λ_g and λ_q increase with increasing μ^2, see Fig. 13 of [1].

3.4 Application to $\gamma^* p \to Vp$

The above results are exactly what we need to describe vector meson production at HERA at large $\gamma^* p$ c.m. energies W. From (6) we see that x_1 is small and $x_2 \approx 0$, that is $x \approx \xi$. The gluon is the relevant parton and the skewed distribution is larger than the conventional gluon by a factor

$$R_g(x=\xi) \;=\; \frac{H_g(\xi,\xi)}{H_g(2\xi,0)} \;=\; \frac{2^{2\lambda_g+3}}{\sqrt{\pi}} \frac{\Gamma\left(\lambda_g + \frac{5}{2}\right)}{\Gamma(\lambda_g+4)}. \tag{21}$$

The cross section formula (5) may then be expressed in terms of the conventional gluon distribution g,

$$\frac{d\sigma}{dt}(\gamma^* p \to V p)\bigg|_{t=0} \;=\; \ldots \left[R_g x_1 g(x_1,\mu^2)\right]^2, \tag{22}$$

where all the off-diagonal effects are contained in the known (enhancement) factor R_g^2. Of course to calculate the cross section properly we must use the unintegrated gluon distribution and integrate over the transverse momenta of the exchanged gluons and of the q and $\bar{q}$ forming the vector meson, see [14].

To obtain the scale dependence of R_g, we first obtain the μ^2 dependence of λ_g of (18) from the behaviour of the gluon found in the global parton analyses. For example, the MRST partons [1] have $\lambda_g = 0.205$ and 0.38 at $\mu^2 = 4$ and 100 GeV^2 respectively. The appropriate scale for the diffractive process $\gamma^*(Q^2)p \to V(q\bar{q})p$ is $\mu^2 \simeq m_q^2 + Q^2/4$. In this way, for diffractive J/ψ and Υ photoproduction at HERA we find from (21) that the off-diagonal enhancement, R_g^2, is $(1.15)^2$ and $(1.32)^2$ respectively. However, for Υ photoproduction, x is not sufficiently small (~ 0.01) and we have to improve the assumption made in (18). If we take $xg \sim x^{-\lambda_g}(1-x)^6$ and perform the x' integration in (15) numerically, then we find an enhancement of $(1.41)^2$ for Υ photoproduction [25]. Moreover note that the skewedness, and hence the enhancement, increase with Q^2. This is particularly noticeable in $\gamma^* p \to \rho p$, see [14].

3.5 Validity of the skewed $\to$ diagonal parton connection

Before we can be sure that the skewed distribution $H(x,\xi)$, at any scale, is fully determined at small x, ξ by knowledge of the diagonal parton distribution, at the same scale, we must consider the points below. First, we have checked that the analytic continuation of the conformal moments O_N in N is allowed [24]. A second consideration is that, from a formal point of view, we may add to the off-diagonal distribution any function which exists only in the ERBL-like region, $|x| < \xi$. In [24] we show such a contribution is negligible $O(\xi^2)$ at small ξ. So far our distributions allow the calculation of the imaginary part of the amplitude for the process. At small x and ξ it turns out that the real part may be calculated easily using a dispersion relation in the c.m. energy squared, W^2, and that the amplitude

$$A \;=\; i\mathrm{Im}A\,\frac{1+e^{-i\pi\lambda}}{1+\cos\pi\lambda}, \tag{23}$$

where $A \propto (W^2)^\lambda$. Finally we note that our result remains valid at NLO, since there is no conformal mixing for $\xi^2 \ll 1$.

3.6 Conclusions

We conclude that, at small x, ξ, the skewed distributions $H(x,\xi;\mu^2)$ are completely known in terms of conventional partons. Thus data for processes which

are described by such distributions can, in principle, be included in a conventional global analysis to better constrain the low x behaviour of the partons. In particular, data for diffractive vector meson production, $\gamma^* p \to Vp$, which depend on the *square* of the gluon distribution, have the potential to put a tight constraint on the gluon at small x. Before this can be done it is necessary to calculate the NLO contributions. Finally here we have been concerned only with the skewed distributions in the small x domain. Skewed distributions, in general, have become an area of intense activity with a large literature (see, for example, [16,26,27] and references therein).

Acknowledgements

I thank Bernd Kniehl, Günter Grindhammer and Gustav Kramer for their efficient organisation of the Ringberg Workshop. I also thank Krzysztof Golec-Biernat, Dick Roberts, Misha Ryskin, Andrei Shuvaev, James Stirling, Thomas Teubner and Robert Thorne for enjoyable collaborations on the subject of this review.

References

1. A.D. Martin, R.G. Roberts, W.J. Stirling and R.S. Thorne, Eur. Phys. J. **C4** (1998) 463.
2. A.D. Martin, R.G. Roberts, W.J. Stirling and R.S. Thorne, `hep-ph/9907231`.
3. CTEQ collaboration: H.L. Lai et al., `hep-ph/9903282`.
4. F. Zomer, these proceedings.
5. U.K. Yang and A. Bodek, Phys. Rev. Lett. **82** (1999) 2467.
6. W. Melnikchouk and A.W. Thomas, Phys. Lett. **B377** (1996) 11.
7. B. Harris, these proceedings.
8. R.S. Thorne and R.G. Roberts, Phys. Rev. **D57** (1998) 6781; Phys. Lett. **B421** (1998) 303.
9. M.A.G. Aivazis, J.C. Collins, F.I. Olness and W.-K. Tung, Phys. Rev. **D50** (1994) 3102.
10. E866 collaboration: E.A. Hawker et al., Phys. Rev. Lett. **80** (1998) 3715; D. Isenhower, Proc. of DIS99, Zeuthen.
11. V. Monaco, these proceedings.
12. W.L. van Neerven et al., Nucl. Phys. **B345** (1990) 331; **B359** (1991) 343; **B382** (1992) 11.
13. J. Blümlein et al., Proc. of 1995/6 HERA Physics Workshop, eds. G. Ingelman et al., Vol. 1, p.23, `hep-ph/9609400`.
14. T. Teubner, these proceedings.
15. A.D. Martin and M.G. Ryskin, Phys. Rev. **D57** (1998) 6692.
16. X. Ji, Phys. Rev. Lett. **78** (1997) 610; Phys. Rev. **D55** (1997) 7114; J.Phys. **G24** (1998) 1181.
17. K. Golec-Biernat and A.D. Martin, Phys. Rev. **D59** (1999) 014029.
18. A.V. Efremov and A.V. Radyushkin, Phys. Lett. **B94** (1980) 245.
19. G.P. Lepage and S.J. Brodsky, Phys. Rev. **D22** (1980) 2157.
20. M. Chase, Nucl.Phys. **B174** (1980) 109.

21. Th. Ohrndorf, Nucl.Phys. **B198** (1982) 26.
22. A.P. Bukhvostov, G.V. Frolov, L.N. Lipatov and E.A. Kuraev, Nucl.Phys. **B258** (1985) 601.
23. A. Shuvaev, `hep-ph/9902318`.
24. A. Shuvaev, K. Golec-Biernat, A.D. Martin and M.G. Ryskin, Phys. Rev. **D60** (1999) 014015.
25. A.D. Martin, M.G. Ryskin and T. Teubner, Phys.Lett. **B454** (1999) 339.
26. A.V. Radyushkin, Phys. Rev. **D56** (1997) 5524.
27. P.A.M. Guichon and M. Vanderhaeghen, Prog. Part. Nucl. Phys. **41** (1998) 125.